
Study of optical absorption in $\text{TlGaSe}_2\text{:Zn}^{2+}$ single crystals

¹Makhnovets G.V., ¹Myronchuk G.L., ²Piskach L.V., ¹Vidrynskyi B.V. and ¹Kevshyn A.H.

¹ Department of Physics, Lesya Ukrainka Eastern European National University, 13 Voli Avenue, 43025 Lutsk, Ukraine

² Department of Inorganic and Physical Chemistry, Lesya Ukrainka Eastern European National University, 13 Voli Avenue, 43025 Lutsk, Ukraine

Received: 19.12.2017

Abstract. We report the results of experimental studies for the optical absorption in $\text{TlGaSe}_2\text{:Zn}^{2+}$ single crystals grown using a modified Bridgman–Stockbarger technique. The absorption measurements at different temperatures are performed with the steps 50 K. The analysis of the experimental data yield in the absorption coefficients of $\text{TlGaSe}_2\text{:Zn}$ varying from 20 to 800 cm^{-1} in the temperature region 100–300 K. Direct and indirect bandgap values for $\text{TlGaSe}_2\text{:Zn}^{2+}$ are calculated as functions of temperature. These values are respectively equal to 2.22 and 2.04 eV at 100 K. It is revealed that the spectral dependences of the absorption coefficient in the region 60–130 cm^{-1} follow the Urbach rule, whereas the corresponding steepness parameter and the Urbach energy increase with increasing temperature.

Keywords: chalcogenides, Urbach energy, direct and indirect bandgaps, steepness parameter

PACS: 42.25.Bs

UDC: 535.343.2

1. Introduction

Physical properties of layered crystalline materials are extensively studied owing to their promising practical applications [1, 2]. These crystals consist of layers with strong (covalent) bonds among the atoms within the layers, whereas much weaker bonds among the layers are mainly of a van der Waals type, which leads to expressed anisotropy of different properties of the crystals and easy formation of structural defects [3]. Up to date, a large number of binary and ternary layered semiconductor structures have been studied in this respect, including InSe, GaSe, GaTe, TlInSe_2 , TlInS_2 and TlGaSe_2 . They have already proved their applicability for many optoelectronic devices [4]. In particular, thallium chalcogenides attract much attention due to their low dimensionality, as well as interesting photoconductive properties, memory effects and optical second-harmonic generation [5–8].

TlGaSe_2 belongs to the group of layered semiconductor compounds of $A^{\text{III}}B^{\text{III}}C_2^{\text{VI}}$ family. It is characterized by a high photosensitivity in the visible spectral range, large birefringence, and a wide optical transparency ranging from 0.6 to 16 μm . TlGaSe_2 crystallizes in the monoclinic group $C2/c$ (No 15), with $Z=16$ and the unit-cell parameters $a=10.779(2)$ Å, $b=10.776(1)$ Å, $c=15.663(5)$ Å, and $\beta=99.993(6)^\circ$ [9]. Each crystalline layer in the structure consists of tetrahedral nodes $[\text{GaSe}_4]$ with strong covalent bonding which has anionic character. The adjusting layers in the elementary cell along the [001] direction are twisted by 90° with respect to each other, thus forming trigonal prismatic voids. Tl cations are located in these voids and connect different layers [10]. It is worthwhile that the formation of defect states in the bandgap of TlGaSe_2

crystals, which can occur with participation of different chemical elements, still remains unclear though it is known that TlGaSe₂ provides the *p*-type conductivity under any doping conditions [11]. It has been suggested that the admixture atoms tend to become separated and self-compensated for a large number of packing defects [12].

It is well-known that such features as a deviation from stoichiometry, availability of impurities, inclusions of different phases or dislocations can notably affect the properties of semiconductor crystals and even cause the appearance of novel physical effects. In other words, the introduction of dopants is an important practical way to change the physical characteristics of semiconductors. On the other hand, defects and impurities can limit significantly the efficiency of practical usefulness of these materials. This justifies comprehensive studies of doped layered semiconductor crystals. Earlier, a wide range of values have been reported for the direct and indirect bandgap energies for the layered TlGaSe₂ crystals (respectively 1.83–2.13 eV and 2.00–2.23 eV [3, 4, 13]). Their optical properties have been described for the wavelength region 200–2000 nm [3]. In particular, it has been shown that the optical absorption in the photon-energy region 30–150 cm⁻¹ and the temperature region 4.2–293 K obeys a well-known Urbach rule. Moreover, abnormal behaviour of the quantitative parameters of this phenomenological model has indicated to a presence of two additional phase transitions in TlGaSe₂ that occur at 246 and 101 K, besides of the transitions earlier established at 120 and 107 K [1, 14, 15]. Apart from the direct and indirect transmission bands and the temperature points of phase transitions, the previous investigations on the subject have also been concerned with the phonon energy, the temperature coefficient and the so-called ‘steepness’ parameter of the Urbach energy, as well as the Debye parameter of A^{III}B^{III}C₂^{VI} single crystals [4, 16–19].

Below we report on the optical properties of Zn-doped TlGaSe₂ crystals and compare them with those typical for pure TlGaSe₂. Our primary aim is elucidating the influence of Zn doping on the characteristics of optical absorption edge and the parameters of the Urbach rule.

2. Experimental

TlGaSe₂ and TlGaSe₂:Zn (2 mol. % of ZnSe) crystals were grown using a horizontal version of a Bridgman–Stockbarger technique. Single-crystalline ingots of TlGaSe₂ and TlGaSe₂:Zn obtained by us were approximately 75 mm long. The samples for optical studies were obtained via splitting the ingots along the cleavage planes. Freshly cleaved crystals had mirror surfaces and did not require further processing. Our optical experiments used a non-polarized light and geometry of light incidence nearly normal to the layers. Optical transmission measurements were performed on 58 and 61 μm thick samples in the temperature region 100–300 K, with the steps of 50 K. A standard nitrogen cryostat and an UTREX K41-3 thermostat were employed to change and control sample temperature (the accuracy ±0.02 K). An MDR-206 monochromator was used in the spectral studies (the wavelength range 360–1100 nm and the resolution ±0.2 nm).

The bandgap energies and the interband optical transitions were studied issuing from experimental spectral dependences of the optical absorption coefficient α . This was done at 100, 150, 200, 250 and 300 K. The α parameter as a function of photon energy $h\nu$ was calculated from the optical transmission measurements, using the formula [20]

$$T = \frac{(1-R)^2 \exp(-\alpha d)}{1-R^2 \exp(-2\alpha d)}. \quad (1)$$

In Eq. (1), $T = I/I_0$ is the transmission coefficient, R the reflection coefficient ($R = 0.2605$)

[21], α the absorption coefficient (measured in cm^{-1}), and d the sample thickness. Note that, for all the temperatures under study, we used the R values known for the room temperature, since the R coefficient changes only slightly from 10 to 320 K [21]. To eliminate multiple light reflections and the corresponding interference fringes, the samples were inclined at a small angle with respect to the normal to the incident beam.

3. Results and discussion

Typical optical absorption spectra obtained for $\text{TlGaSe}_2\text{:Zn}$ are presented in Fig. 1. The analysis of the experimental data yields the absorption coefficients varying from 20 to 800 cm^{-1} in the region of 100–300 K. If compared with TlGaSe_2 , the spectra are shifted towards the lower-energy region [21]. Note that the shape of the absorption edge is complex enough. So, at 100 K one observes the absorption bands with the maxima located at $\sim 2.13 \text{ eV}$ and $\sim 2.18 \text{ eV}$ respectively for TlGaSe_2 and $\text{TlGaSe}_2\text{:Zn}$. The peaks exhibit noticeable thermal broadening with increasing temperature.

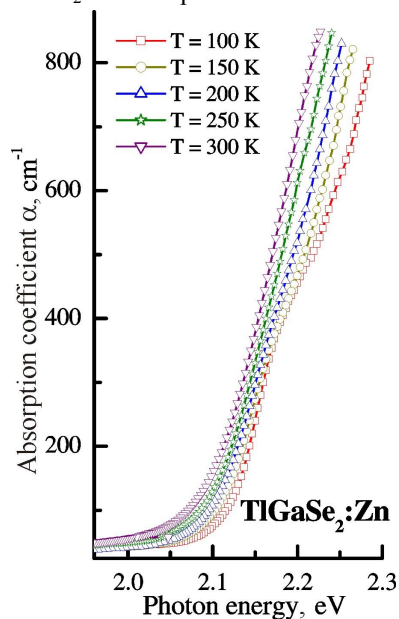


Fig. 1. Typical absorption spectra measured for the $\text{TlGaSe}_2\text{:Zn}$ crystals at 100, 150, 200, 250 and 300 K.

It is important that some transitions involving the levels associated with defects and excitons are observed in the absorption spectra of p - TlGaSe_2 single crystals at the temperatures below 120 K [22]. The relevant bands are broader but still present in the spectra recorded at 200 K [23]. It is known that, at 10 K, p - TlGaSe_2 has three different peaks at 2.131, 2.159 and 2.208 eV [5], while p - $\text{TlGa}_{0.999}\text{Pr}_{0.001}\text{Se}_2$ exhibits two peaks with the energies 2.144 and 2.174 eV at the same temperature. The peaks located at 2.159, 2.174 and 2.208 eV have been ascribed to the excitons, while that located at 2.131 eV disappears in a Pr-doped p - TlGaSe_2 sample, being accompanied with lower absorption coefficients. To elucidate the nature of the absorption band at $\sim 2.18 \text{ eV}$ observed in our study for $\text{TlGaSe}_2\text{:Zn}$, the investigations at still lower temperatures are required.

As shown in Ref. [24], the TlGaSe_2 crystals usually deviate significantly from the stoichiometry conditions. The deficits of thallium and gallium are respectively 1.54 and 1.12 at. %, while the excess of selenium amounts to 2.71 at. %. The excessive concentrations of cation vacancies create favourable conditions for the formation of creep dislocations, causing spiral twisting. The investigations of the forms and numbers of inclusions in TlGaSe_2 [24] have led to the conclusion that there are linear defects in which segregation of impurities takes place. The segregation of super-stoichiometric selenium may follow the similar way. Any deviation from the periodic

arrangement of atoms in their lattice sites would lead to formation of a random potential relief of the edges of allowed bands and appearance of tail of the density of states in the bandgap. It is the light absorption with participation of the density-of-states tail that causes tailing of the fundamental absorption edge.

It has been shown both experimentally and theoretically that the exponential edge characterized by the Urbach rule can arise from both phonon dynamics and statistical structural disordering [25]. For high-quality crystalline semiconductors, the Urbach energy is directly linked with the temperature disorder, whereas for amorphous or heavily doped materials, it increases as a result of increasing statistical disorder. The exponential region (i.e., the Urbach tail) for the $\text{TlGaSe}_2\text{:Zn}$ crystals is observed in the region $60\text{--}130\text{ cm}^{-1}$ of the absorption coefficient, which agrees well with the data reported in Ref. [26]. Extrapolation of the absorption dependences on a semi-logarithmic scale at different temperatures forms convergent straight lines, with the convergence point corresponding to the bandgap energy E_{g0} at $T = 0\text{ K}$. The typical Urbach tails observed at a number of temperatures are presented in Fig. 2. Then the absorption plots yield in a ‘convergent’ absorption coefficient. The coordinates E_{g0} and α_0 of this point are 2.23 eV and 1300 cm^{-1} , respectively. This testifies that the absorption spectra of $\text{TlGaSe}_2\text{:Zn}$ follow the Urbach rule.

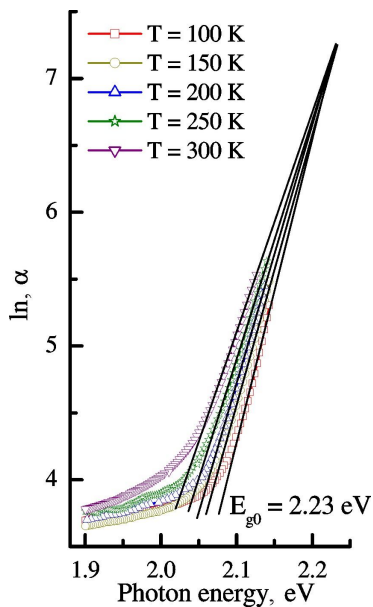


Fig. 2. Typical absorption spectra obtained for the $\text{TlGaSe}_2\text{:Zn}$ crystals at 100, 150, 200, 250 and 300 K.

The problems of physical grounds of the empirical Urbach rule have been repeatedly discussed (see, e.g., Refs. [27, 28]). The majority of the works on the subject explain the exponential edge of spectral absorption dependence by interactions of electrons (excitons) with atomic vibrations in the crystal lattice. A series of studies have been devoted to the analysis of cases of the weak and strong electron(exciton)–phonon interactions [26]. Mahan’s theory is one of the explanations for the appearance of Urbach tail in polar crystals, including ferroelectric materials such as a number of $\text{A}^{\text{III}}\text{B}^{\text{III}}\text{C}^{\text{VI}}_2$ compounds (e.g., TlGaSe_2 , InGaSe_2 , InGaTe_2 and TlGaTe_2) [28]. This theory relates the Urbach tail to the interaction of electrons with longitudinal optical phonons. Besides, random electric fields appearing due to fluctuations of the bulk density of free carriers affect substantially the shape of the absorption edge. In Ref. [29] it has been suggested that, as long as the microfields (i.e., phonon-generated changes in the local electric fields) are small enough, the steepness parameter of the Urbach model increases linearly with

temperature, and the slope of the absorption edge remains nearly constant and does not depend on temperature. If this is correct, then the broadening of the absorption edge resulting in the exponential Urbach tail is caused primarily by the structural disorder (e.g., due to charged defects). The both mechanisms would cause local distortions of the valence and conduction bands, thus producing exponential shape of the spectral absorption dependence. Hence, the studies of the temperature dependence of the Urbach tail can yield important information on the interaction of electrons and/or excitons with phonons in our semiconductor crystal.

According to the Urbach rule [30], the exponential dependence of the absorption coefficient α on the photon energy $h\nu$ is expressed as

$$\alpha = \alpha_0 \exp\left[\sigma(h\nu - E_{g0})/kT\right], \quad (2)$$

where $h\nu$ is the photon energy, k the Boltzmann constant, T the sample temperature, $\sigma(T)$ the ‘steepness’ parameter of the absorption edge, $kT/\sigma(T) = E_U$ the characteristic Urbach energy, whereas α_0 and E_{g0} are the coordinates of the convergence point of the functions $\ln \alpha = f(h\nu)$ at different temperatures.

The steepness parameter characterizes the slope of the straight-line absorption plot near the absorption edge. Empirically it can be expressed as a function of temperature [27, 31]:

$$\sigma(T) = \sigma_0 (2kT/h\nu_p) \tanh(h\nu_p/2kT), \quad (3)$$

where $h\nu_p$ is the average energy of phonons related to the Urbach tail [32] and σ_0 the temperature-independent material-specific parameter, which is inversely proportional to the force g of the interaction of electrons (or excitons) with phonons [27]:

$$g = 2/3 \sigma_0^{-1}. \quad (4)$$

The Urbach energy E_U that corresponds to the reverse slope of the Urbach tail and the steepness parameter σ are plotted as functions of temperature in Fig. 3. The Urbach energy and the steepness parameter increase with increasing temperature, as listed in Table 1. We suggest that this fact is related to recharging of defect centres because lower temperatures neutralize partially the charged centres and decrease their effect on the random modulation of electric field in a sample [33].

The temperature-dependent steepness parameter, which can be calculated from the slope of the Urbach tails, is presented in Fig. 3 by open dots. To evaluate the energy of the phonons related to the Urbach tails, the experimental results have been fitted using Eq. (3) with σ_0 and $h\nu_p$ as free parameters. The fits are plotted in Fig. 3 by solid lines. We obtain $\sigma_0 = 0.58$ and 0.56 , and $h\nu_p = 42$ and 51 ± 1.0 meV for TlGaSe_2 and $\text{TlGaSe}_2\text{:Zn}$, respectively.

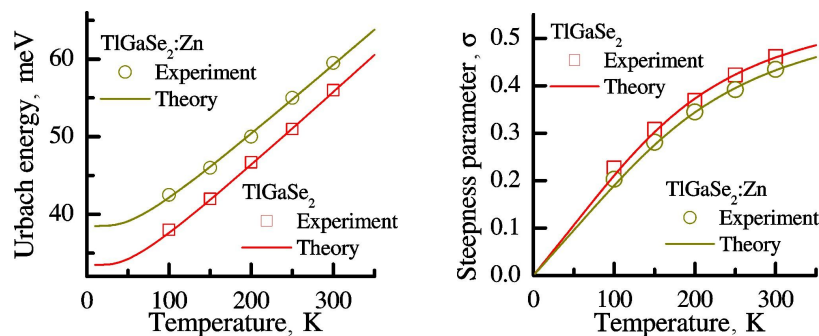


Fig. 3. Urbach energy and steepness parameter as functions of temperature, as calculated for the TlGaSe_2 and $\text{TlGaSe}_2\text{:Zn}$ crystals. Solid lines correspond to fitting performed with Eq. (4).

Table 1. Urbach energy and steepness parameter calculated for the TlGaSe₂ and TlGaSe₂:Zn crystals at different temperatures.

Sample temperature, K	Crystal			
	TlGaSe ₂		TlGaSe ₂ :Zn	
	Urbach energy, meV	Steepness parameter	Urbach energy, meV	Steepness parameter
100	38	0.227	52	0.166
150	44	0.294	55	0.235
200	49	0.352	60	0.287
250	56	0.385	64	0.337
300	59	0.438	68	0.380

The phonon modes in TlGaSe₂ have earlier been observed in the region of 50.5–275.7 cm⁻¹ (i.e., 7–36 meV), using the Raman studies [34]. These energies are lower than the $h\nu_p$ values obtained from our experimental data. A higher $h\nu_p$ value obtained for the II–VI compounds with the zinc-blend structure is related to higher symmetry of these crystals. On the other hand, in the ternary chalcopyrite compounds and mixed chalcogenides, it is related to the structural deviations caused by cation disorder (cation vacancies, interstitial atoms, etc.) and deviation from the ideal stoichiometry. Notice also that the σ_0 constant for TlGaSe₂:Zn²⁺ is lower than that for TlGaSe₂. This parameter is inversely proportional to the force of phonon bonding, which indicates that the electron(exciton)–phonon interactions in TlGaSe₂:Zn are stronger than those occurring in TlGaSe₂. The decrease of σ_0 observed in the TlGaSe₂ crystals can be associated with the introduction of Zn. Indeed, it represents a charged admixture and so affects the electron(exciton)–phonon interactions. The g parameters obtained from Eq. (4) are equal to 1.15 and 1.18 respectively for the TlGaSe₂ and TlGaSe₂:Zn crystals. These values are typical for the crystals having nonstoichiometric defects in the cation sublattice.

The temperature dependence of the Urbach energy is often used for estimating the prevailing mechanisms that contribute to tailing of the fundamental absorption edge. As seen from Table 1, the Urbach energy in the temperature region 100–300 K varies from 38 to 56 meV for TlGaSe₂ and from 43 to 60 meV for TlGaSe₂:Zn. It has been established that E_U can be modelled in terms of an Einstein oscillator that combines the contribution of dynamic (thermal) and statistical (structural and compositional) deviations in a sample [25]. According to this model, the Urbach energy can be expressed as follows:

$$E_U = A \left(1 / \left(e^{\Theta/T} - 1 \right) \right) + B, \quad (5)$$

where A and B are the constants linked with the thermal and statistical (structural and compositional) disorders, Θ denotes the Einstein temperature related to the Debye temperature Θ_D as $\Theta \approx 3/4 \Theta_D$ [4]. Finally, the Debye temperatures estimated from the appropriate dependences for TlGaSe₂ and TlGaSe₂:Zn are 203 and 217±2 K, which agrees well with the data of Ref. [16].

Eq. (5) means that the Urbach energy depends additively on the electron–phonon interactions and the structural disorder. According to Ref. [25], we have

$$E_U = k \left[\left\langle U^2 \right\rangle_T \right] + k \left[\left\langle U^2 \right\rangle_X \right], \quad (6)$$

where $\langle U^2 \rangle_T$ and $\langle U^2 \rangle_X$ are the mean-square offsets of atoms from their equilibrium lattice sites, which are caused respectively by the dynamic and statistical disorders.

The first term in the r. h. s. of Eq. (6) represents a contribution of the electron–phonon interactions as a Debye–Waller factor, while the second term results from the mean-square shift of atoms caused by the structural deviation from an ideally ordered lattice. The experimental data displayed in Fig. 3 can be fitted by a straight line obtained from Eq. (5). The fitting parameters are equal to $A = 14.7$ meV and $B = 33.5$ meV for TlGaSe_2 , and $A = 15$ meV and $B = 38.5$ meV for $\text{TlGaSe}_2\text{:Zn}^{2+}$. Considering these A and B values, one can conclude that the structural and composition deviations (B) dominate in the entire temperature range, since their contribution into the Urbach energy is higher than that of the thermally induced disorder (A). The increase in the parameter B found for the $\text{TlGaSe}_2\text{:Zn}^{2+}$ crystals, if compared with TlGaSe_2 , can be explained by increasing contribution of the static disorder related to higher concentration of structural defects. This result implies that the phonon energy $\hbar\nu_p$, which corresponds to the energy of the highest optical mode or the average for these modes, is related to the structural and compositional disorders.

More detailed information on the bandgap energy can be obtained from the analysis of dependence of the absorption coefficient on the photon energy. The absorption coefficient above the exponential tail is described by the relation

$$\alpha \hbar\nu = B(\hbar\nu - E_g)^N, \quad (7)$$

where B is the proportionality coefficient dependent on the probability of optical transitions, and N denotes the index that characterizes the corresponding processes [It can acquire the values $1/2$, $3/2$, 2 or 3 , depending on the nature of electron transitions responsible for the absorption]. The N values in the above sequence correspond respectively to the direct allowed (high-energy part of the spectrum), direct forbidden, indirect allowed (low-energy spectral region) and indirect forbidden transitions [35].

The analysis of the experimental results shown in Fig. 1 indicates that both the direct and indirect allowed transitions occur in the $\text{TlGaSe}_2\text{:Zn}$ crystals. The coexistence of these transitions in the $\text{A}^{\text{III}}\text{B}^{\text{III}}\text{C}_2^{\text{VI}}$ crystals has earlier been reported in Refs. [1, 16, 17, 36, 37]. We have obtained the direct and indirect bandgap energies for $\text{TlGaSe}_2\text{:Zn}$ from the dependences $(\alpha\hbar\nu)^2 = f(\hbar\nu)$ and $(\alpha\hbar\nu)^{1/2} = f(\hbar\nu)$ by extrapolating their linear parts to the abscissa axis at $(\alpha\hbar\nu)^2 = 0$ and $(\alpha\hbar\nu)^{1/2} = 0$ (see Fig. 4a, b). The direct and indirect bandgap energies for the $\text{TlGaSe}_2\text{:Zn}$ crystals are listed in Table 2 for the temperatures 100, 150, 200, 250 and 300 K. It is known that the doping leads to decrease in both the direct and indirect bandgaps, when compared to the pure TlGaSe_2 crystals [16]. Moreover, it has been found in Ref. [21] that the difference between the direct and indirect bandgap energies is equal to 0.15 eV at the room temperature, which agrees well with our results.

Table 2. Direct (E_g^d) and indirect (E_g^i) bandgap values obtained for the $\text{TlGaSe}_2\text{:Zn}$ crystals at different temperatures.

Crystal	Temperature, K	E_g^d , eV	E_g^i , eV
TlGaSe ₂ :Zn	100	2.22	2.04
	150	2.21	2.03
	200	2.19	2.02
	250	2.18	2.01
	300	2.16	2.00

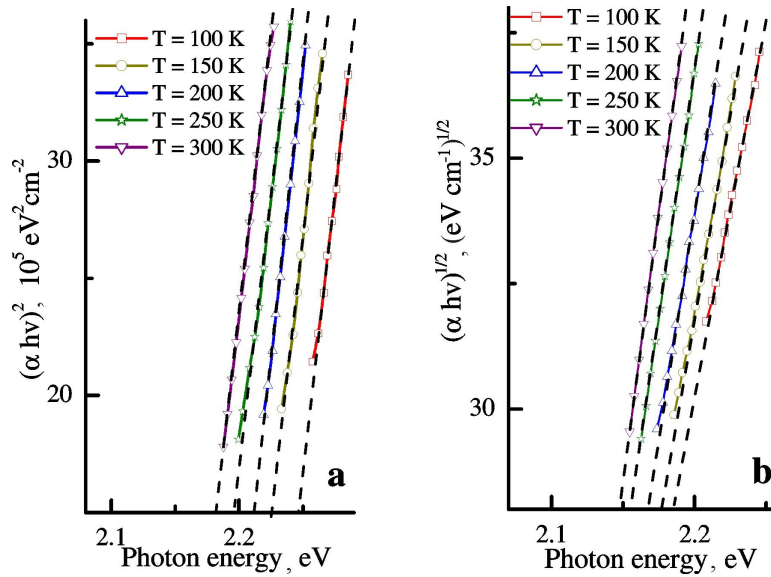


Fig. 4. Experimental dependences that illustrate direct-transition (a) and indirect-transition (b) mechanisms of the absorption spectra in TiGaSe₂:Zn.

Temperature dependences of the direct and indirect bandgap energies for the TiGaSe₂:Zn crystals are presented in Fig. 5 and Table 2. It is evident that both the direct and indirect bandgaps decrease with increasing temperature. The temperature coefficients ($\delta = dE_g/dT$) for the direct and indirect bandgaps have been calculated as $-3 \cdot 10^{-4}$ and $-2 \cdot 10^{-4}$ eV/K, respectively. These results agree well with the data reported in Ref. [1]. The parameter dE_g/dT depends on the expansion of crystal lattice and on the electron–phonon interactions [38]. This dependence is described as

$$\frac{dE_g}{dT} = \left(\frac{dE_g}{dT} \right)_l + \left(\frac{dE_g}{dT} \right)_{e-p}, \quad (8)$$

where the first and second terms refer respectively to the lattice expansion and the electron–phonon interactions.

Notice that the sign of the temperature coefficient involved in Eq. (8) does not depend on the sign of either of the terms. Instead, it depends on the nature of the system. It is known that the temperature coefficients for the indirect and direct bandgaps have the negative sign, which indicates larger contribution of the term corresponding to the electron–phonon interactions than that of the crystal-lattice expansion. At the same time, the decrease observed in the direct and indirect

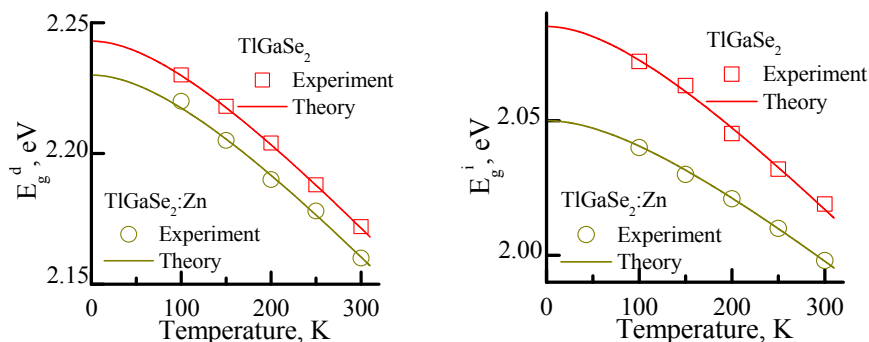


Fig. 5. Temperature dependences of direct (E_g^d) and indirect (E_g^i) bandgap values obtained for the TiGaSe₂ and TiGaSe₂:Zn crystals. Solid lines correspond to the fits with Eq. (9).

bandgaps with increasing temperature is a typical feature for the crystals with layered structure [36, 37]. It should also be noted that some representatives of the $A^{III}B^{III}C_2^{VI}$ family, e.g. $TlInTe_2$ and $TlInSe_2$, demonstrate a positive temperature slope of the bandgap-energy variation [23].

The temperature dependence of the bandgap can be presented using the empirical relationship suggested by Varshni [39]:

$$E_g(T) = E_g(0) - \delta \frac{T^2}{T + \beta}. \quad (9)$$

Here E_{g0} is the bandgap energy at 0 K, δ the temperature rate of the bandgap variation, and β the parameter close to the Debye temperature. One can notice a fairly good agreement of the parameter β and the Debye temperature found earlier for the $Tl_2In_2S_3Se$ crystals. It has been estimated with the Lindemann melting rule, using the X-ray data and the melting point $T_m = 1048$ K [19]. The solid lines in Fig. 5 show the best fits of the experimental temperature dependences of the bandgap. The fitting parameters $E_{gd0} = 2.23$ eV, $E_{gi0} = 2.05$ eV, $\beta = 217$ K, and $\delta = 4 \cdot 10^{-4}$ and $3 \cdot 10^{-4}$ eV/K are obtained, where the two latter results refer respectively to the direct allowed and indirect allowed transitions. These parameters agree well with the experimental data obtained in the present work.

4. Conclusion

In the present work, we have performed optical studies of the $TlGaSe_2:Zn$ single crystals grown by the Bridgman–Stockbarger technique. It has been found that the spectral dependences of the absorption coefficient in the region $60\text{--}130\text{ cm}^{-1}$ follow the Urbach rule at the temperatures ranging from 100 up to 300 K. The temperature dependence of the Urbach energy agrees well with a simple empirical model. In addition to the effect of electron(exciton)–phonon interactions, this model takes into consideration the local electric field distortions that lead to higher phonon energies due to the structural and compositional disorderings.

The structural disordering in our crystals is likely related to the presence of numerous structural defects such as 2D dislocations and packing defects in the $TlGaSe_2:Zn$ lattice, which has earlier been observed for the other layered materials. The parameters obtained from the phenomenological relations have provided us with the estimates of the bandgap, the Debye temperature, the strength of electron–phonon interactions, and the mean energy of phonons related to the Urbach tails. The data obtained in this work can be potentially useful for the band-structure studies and judging possible applications of $TlGaSe_2:Zn$ in optoelectronics.

References

1. Gürbulak B and Duman S, 2008. Urbach tail and optical characterization of gadolinium-doped $TlGaSe_2$ single crystals. *Phys. Scripta*. **77**: 025702.
2. Youssef S B, 1995. Phase transitions and electrical conductivity of $TlInS_2$. *Physica A*. **215**: 176–180.
3. El-Nahass M M, Sallam M M, Samy A R and Ibrahim E M, 2006. Optical, electrical conduction and dielectric properties of $TlGaSe_2$ layered single crystal. *Solid State Sci*. **8**: 488–499.
4. Abay B, Guder H S, Efeoglu H and Yogurtcu Y K, 2001. Temperature dependence of the optical energy gap and Urbach–Martienssen’s tail in the absorption spectra of the layered semiconductor $Tl_2GaInSe_4$. *J. Phys. Chem. Sol.* **62**: 747–752.
5. Guler I, Ambrico M, Ligonzo T and Gasanly N M, 2013. Temperature-dependent absorption edge and photoconductivity of $Tl_2In_2S_3Se$ layered single crystals. *J. Alloys Comp.* **550**: 471–474.

6. Panich A M and Sardarly R M, 2010. Physical properties of the low-dimensional A^3B^6 and $A^3B^3C^6_2$ compounds. New York: Nova Science Publishers.
7. Seyidov M Yu, Sahin Y, Erbahar D and Suleymanov R A, 2006. Electret states and current oscillations in the ferroelectric semiconductor $TlGaSe_2$. *Phys. stat. sol. (a)*. **203**: 3781–3787.
8. Panich A M, Ailion D C, Kashida S and Gasanly N, 2004. Gallium and thallium NMR study of phase transitions and incommensurability in the layered semiconductor $TlGaSe_2$. *Phys. Rev. B*. **69**: 245319.
9. Delgado G E, Mora A J, Pérez F V and González J, 2007. Growth and crystal structure of the layered compound $TlGaSe_2$. *Cryst. Res. Technol.* **42**: 663–666.
10. Ves S, 1989. Effects of hydrostatic pressure on the fundamental absorption edge of $TlGaSe_2$. *Phys. Rev. B*. **40**: 7892–7897.
11. Senturk E, Tumbek L and Mikailov F A, 2005. Dielectric properties of thallium gallium diselenide crystal in the incommensurate phase. *Cryst. Res. Technol.* **40**: 901–904.
12. McMorro D F, Cowley R A, Hatton P D and Banys J, 1990. The structure of the paraelectric and incommensurate phases of $TlGaSe_2$. *J. Phys.: Condens. Matter*. **2**: 3699.
13. Ozdemir S and Bucurgat M, 2014. Photoelectrical properties of $TlGaSe_2$ single crystals. *Solid State Sci.* **33**: 25–31.
14. Allakhverdiev K R, Aldzhonov M A, Mamedov T G and Salaev E Yu, 1986. Anomalous behaviour of the Urbach edge and phase transitions in $TlGaSe_2$. *Sol. State Commun.* **58**: 295–297.
15. Durnev Yu I, Kulbuzhev B S, Malsagov A U, Rabkin L M, Torgashev V I and Yuzyk Yu I, 1989. Vibrational spectra and phase transitions in layered semiconducting ferroelectrics with $TlGaSe_2$ structure. I. Temperature dependences of parameters of the Raman spectrum lines of $TlGaSe_2$. *Phys. stat. sol. (b)*. **153**: 517–527.
16. Duman S and Gürbulak B, 2005. Urbach tail and optical absorption in layered semiconductor $TlGaSe_{2(1-x)}S_{2x}$ single crystals. *Physica Scripta*. **72**: 79–86.
17. Gürbulak B, 1999. Growth and absorption properties of Dy-doped and undoped p-type $TlGaSe_2$. *Appl. Phys. A*. **68**: 353–356.
18. Grivickas V, Gavryushin V, Grivickas P, Galeckas A, Bikbajevs V and Gulbinas K, 2011. Optical absorption related to Fe impurities in $TlGaSe_2$. *Phys. stat. sol. (a)*. **208**: 2186–2192.
19. Guler I, Ambrico M, Ligonzo T and Gasanly N M, 2013. Temperature dependent absorption edge and photoconductivity of $Tl_2In_2Se_3S$ layered single crystals. *J. Alloys Comp.* **550**: 471–474.
20. Moss T S, Optical process in semiconductors. London: Butterworths. (1959).
21. Haniyas M, Anagnostopoulos A, Kambas K and Spyridelis J, 1989. On the non-linear properties of $TlInX_2$ ($X = S, Se, Te$) ternary compounds. *J. Phys. B*. **160**: 154–160.
22. Gurbulak B, 2001. The optical investigation of $TlGa_{0.999}Pr_{0.001}Se_2$ and $TlGaSe_2$ single crystals. *Physica B: Cond. Mater* **293**: 289–296.
23. Kalomirois J A, Kalkan N, Haniyas M, Anagnostopoulos A N and Kambas K, 1995. Optical and photoelectric properties of $TlGaSe_2$ layered crystals. *Sol. State Commun.* **96**: 601–607.
24. Guseinov G D, Aliyev V A and Bagirzade E F, 1985. Defects in $TlGaSe_2$. *Mater. Chem. Phys.* **13**: 541–550.
25. Yang Z, Homewood K P, Finney M S, Harry M A and Reeson K J, 1995. Optical absorption study of ion beam synthesized polycrystalline semiconducting $FeSi_2$. *J. Appl. Phys.* **78**: 1958–1963.

26. Cody G D, Tiedje T, Abeles B, Brooks B and Goldstein Y, 1981. Disorder and the optical absorption edge of hydrogenated amorphous silicon. *Phys. Rev. Lett.* **47**: 1480–1483.
27. Kurik M V, 1971. Urbach rule. *Phys. stat. sol. (a)*. **8**: 9–45.
28. Mahan G D, 1966. Phonon-broadened optical spectra: Urbach's rule. *Phys. Rev.* **145**: 602–608.
29. Brada Y and Roth M, 1989. Optical absorption of $\text{KTa}_{1-x}\text{Nb}_x\text{O}_3$ single crystals. *Phys. Rev. B*. **39**: 10402–10405.
30. Urbach F, 1953. The long-wavelength edge of photographic sensitivity and of the electronic absorption of solids. *Phys. Rev.* **92**: 1324.
31. Martienssen H W, 1957. Über die excitonenbanden der alkalihalogenidkristalle. *J. Phys. Chem. Sol.* **2**: 257–267.
32. Sumi H and Toyozawa Y, 1971. Urbach-Martienssen rule and exciton trapped momentarily by lattice vibrations. *J. Phys. Soc. Japan*. **31**: 342–358.
33. Myronchuk G L, Davydyuk G E, Parasyuk O V, Khyzhun O Y, Andrievski R A, Fedorchuk A O, Danylchuk S P, Piskach L V and Mozolyuk M Yu, 2013. $\text{Tl}_{1-x}\text{In}_{1-x}\text{Sn}_x\text{Se}_2$ ($x = 0, 0.1, 0.2, 0.25$) single-crystalline alloys as promising non-linear optical materials. *J. Mater. Sci: Mater. Electron.* **24**: 3555–3563.
34. Paucar R, Itsuwa H, Wakita K, Shim Y, Alekperov O and Mamedov N, 2015. Phase transitions and Raman scattering spectra of TlGaSe_2 . *J. Phys: Conf. Ser.* **619**: 012018.
35. Pankove J I, 1971. Optical processes in semiconductors. New York: Dover.
36. Piasecki M, Myronchuk G L, Zamurueva O V, Khyzhun O Y, Parasyuk O V, Fedorchuk A O, Albassam A, El-Naggar A M and Kityk I V, 2016. Huge operation by energy gap of novel narrow band gap $\text{Tl}_{1-x}\text{In}_{1-x}\text{B}_x\text{Se}_2$ ($\text{B} = \text{Si}, \text{Ge}$): DFT, x-ray emission and photoconductivity studies. *Mater. Res. Exp.* **3**: 025902.
37. Zamurueva O V, Myronchuk G L, Lakshminarayana G, Parasyuk O V, Piskach L V, Fedorchuk A O, AlZayed N S, El-Naggar A M and Kityk I V, 2014. Structural and optical features of novel $\text{Tl}_{1-x}\text{In}_{1-x}\text{Ge}_x\text{Se}_2$ chalcogenide crystals. *Opt. Mater.* **37**: 614–620.
38. Abdullaeva S G, Abdullaev N A, Belenkii G L, Mamedov N T and Suleimanov R A, 1983. Temperature-induced shift of an exciton band and deformation effects in layered TlGaSe_2 crystals. *Fiz. Techn. Poluprov.* **17**: 1320–1321.
39. Varshni Y P, 1967. Temperature dependence of the energy gap in semiconductors. *Physica* **34**: 149–154.

Makhnovets G. V., Myronchuk G. L., Piskach L. V., Vidrynskyi B. V. and Kevshyn A. H. 2018. Study of optical absorption in $\text{TlGaSe}_2:\text{Zn}^{2+}$ single crystals. *Ukr.J.Phys.Opt.* **19**: 49 – 59.

Анотація. Представлено результати експериментальних досліджень оптичного поглинання монокристалів $\text{TlGaSe}_2:\text{Zn}^{2+}$, вирощених за модифікованим методом Бріджмена–Стокбаргера. Вимірювання поглинання при різних температурах виконано з кроком 50 К. Аналіз даних показав, що коефіцієнт поглинання $\text{TlGaSe}_2:\text{Zn}$ змінюється в межах від 20 до 800 см^{-1} у температурному діапазоні 100–300 К. Прямі та непрямі величини ширини забороненої зони розраховано як функції температури. За температури 100 К ці параметри складають відповідно 2,22 і 2,04 еВ. Встановлено, що спектральні залежності коефіцієнта поглинання в області 60–130 см^{-1} описуються правилом Урбаха, а відповідний параметр крутизни краю поглинання та енергія Урбаха зростають зі зростанням температури.